The Canadian Mineralogist
Vol. 33, pp. 25-31 (1995)

SYNTHESIS AND CRYSTAL-STRUCTURE REFINEMENT OF SYNTHETIC FLUOR-PARGASITE

ROBERTA OBERTI AND NICOLA SARDONE

CNR – Centro di Studio per la Cristallochimica e la Cristallografia, via Abbiategrasso, 209, I-27100 Pavia, Italy

FRANK C. HAWTHORNE, MATI RAUDSEPP* AND ALLAN C. TURNOCK

Department of Geological Sciences, University of Manitoba, Winnipeg, Manitoba R3T 2N2

ABSTRACT

Large crystals of amphibole were synthesized by slow cooling of a bulk composition nominally that of end-member fluor-pargasite. The crystal structure of two fragments of average composition $Na_{0.855}Ca_{2.044}Mg_{0.161}(Mg_{4.227}Al_{0.773})(Si_{5.962}Al_{2.038})O_{22}F_2$, *a* 9.820(4), *b* 17.896(6), *c* 5.294(2) Å, β 105.30(3)°, *V* 897.4(2) Å^3, and $Na_{0.808}Ca_{2.228}Mg_{0.155}(Mg_{4.062}Al_{0.938})(Si_{5.800}Al_{2.200})O_{22}F_2$, *a* 9.808(2), *b* 17.868(5), *c* 5.297(2) Å, β 105.30(2)°, *V* 895.4(2) Å^3, *C2/m*, *Z* = 2, were refined to *R* indices of ~1.3% for ~1050 observed reflections collected with Mo*K*α X-radiation. Tetrahedrally coordinated Al occurs at both *T*(1) and *T*(2), but with Al strongly preferring the *T*(1) site. This observed disorder is consistent with ^{29}Si MAS NMR results on synthetic scandium-fluor-pargasite (Raudsepp *et al.* 1987). Octahedrally coordinated Al is ordered at *M*(2), similar to the ordering scheme in synthetic scandium- and chromium-fluor-pargasite (Raudsepp *et al.* 1987). Both Na and Ca occur at the *A* site in the crystals examined; the pattern of electron density observed suggests that Na is disordered between *A*(*m*) and *A*(2), and that Ca occurs predominantly at *A*(2).

Keywords: amphibole, fluor-pargasite, synthesis, crystal-structure refinement, ordering, electron-microprobe analysis.

SOMMAIRE

Nous avons réussi à synthétiser des cristaux relativement gros d'amphibole en laissant refroidir lentement un mélange ayant la composition globale du pôle fluor-pargasite. La structure cristalline de deux fragments, ayant une composition moyenne $Na_{0.855}Ca_{2.044}Mg_{0.161}(Mg_{4.227}Al_{0.773})(Si_{5.962}Al_{2.038})O_{22}F_2$, *a* 9.820(4), *b* 17.896(6), *c* 5.294(2) Å, β 105.30(3)°, *V* 897.4(2) Å^3, et $Na_{0.808}Ca_{2.228}Mg_{0.155}(Mg_{4.062}Al_{0.938})(Si_{5.800}Al_{2.200})O_{22}F_2$, *a* 9.808(2), *b* 17.868(5), *c* 5.297(2) Å, β 105.30(2)°, *V* 895.4(2) Å^3, *C2/m*, *Z* = 2, respectivement, a été affinée jusqu'à un résidu *R* d'environ 1.3% en utilisant une moyenne de 1050 réflexions observées (rayonnement Mo*K*α). L'aluminium à coordinence tétraédrique est présent dans les sites *T*(1) et *T*(2), mais il préfère fortement le site *T*(1). Le désordre observé concorde avec les résultats d'une étude de la fluor-pargasite synthétique dopée avec le scandium par résonance magnétique nucléaire du ^{29}Si avec spin à l'angle magique (Raudsepp *et al.* 1987). L'aluminium à coordinence octaédrique est ordonné sur *M*(2), comme dans ce matériau et son analogue dopé avec le chrome (Raudsepp *et al.* 1987). Le Na et le Ca occupent le site *A* dans ces deux cristaux. D'après la distribution de la densité des électrons, le Na serait désordonné entre *A*(*m*) et *A*(2), tandis que le Ca occuperait surtout *A*(2).

(Traduit par la Rédaction)

Mots-clés: amphibole, fluor-pargasite, synthèse, affinement de la structure cristalline, mise en ordre, analyse à la microsonde électronique.

INTRODUCTION

Pargasite and its varieties have been popular amphiboles to synthesize during the past twenty years, partly because of their relative ease of synthesis and partly because of their petrological importance. Charles (1980) synthesized amphiboles along the join pargasite – ferro-pargasite and described the behavior of the cell dimensions as a function of composition. Westrich & Navrotsky (1981) synthesized fluor-pargasite and reported cell dimensions and thermodynamic properties. Raudsepp *et al.* (1987) synthesized pargasitic and fluor-pargasitic amphiboles with a variety of trivalent cations at the octahedral sites, $NaCa_2(Mg_4M^{3+})(Si_6Al_2)O_{22}(OH,F)_2$, with M^{3+} representing Al, Cr^{3+}, Ga, Sc, In, and reported cell dimensions,

* Current address: Department of Geological Sciences, University of British Columbia, Vancouver, British Columbia V6T 2B4.

infrared spectra, Rietveld structure-refinements and ^{27}Al, ^{29}Si and ^{19}F magic-angle spinning nuclear magnetic resonance (MAS NMR) spectra. Welch *et al.* (1994) synthesized fluor-pargasite and reported the infrared, multi-nuclear MAS NMR and cross-polarization MAS NMR spectra. Jenkins & Hawthorne (1995) synthesized Ga-pargasite of the form $NaCa_2(Mg_4M^{3+})(Si_6M^{3+}_2)O_{22}(OH)_2$ with M^{3+} representing Al and Ga, and reported cell dimensions and Rietveld structure-refinements.

Of particular interest in these amphiboles is the observation by Raudsepp *et al.* (1987) that ideal end-member pargasite, $NaCa_2(Mg_4Al)(Si_6Al_2)O_{22}(OH)_2$, and its Ga, Cr and Sc analogues show significant disorder of the trivalent octahedrally coordinated cations. The infrared spectrum in the principal hydroxyl-stretching region shows two bands that they interpreted as being due to MgMgMg and MgMgM^{3+} configurations at the $M(1)$ and $M(3)$ sites. At that time, this seemed unlike the behavior of (natural) pargasite (Robinson *et al.* 1973); however, more recent work (Oberti *et al.* 1995) has shown substantial Al occupancy of the $M(3)$ site in Mg-rich pargasite, in agreement with the results of Raudsepp *et al.* (1987) and Welch *et al.* (1994) on synthetic end-member pargasite. Raudsepp *et al.* (1987) also synthesized fluor-pargasite; the <*M*–O> bond-lengths derived from Rietveld refinement suggest that Al is ordered at $M(2)$, but we do not regard this result as definitive, and it is not clear whether there is some Al–Mg disorder at the $M(1)$ and $M(3)$ sites. Rietveld structure-refinement of scandium- and chromium-fluor-pargasite showed M^{3+} to be ordered at $M(2)$, in contrast to the M^{3+} disorder observed in (hydroxy-) pargasite (Raudsepp *et al.* 1987). In addition, the ^{29}Si MAS NMR spectrum of scandium-fluor-pargasite reported by Raudsepp *et al.* (1987) is compatible with significant Al disorder over the $T(1)$ and $T(2)$ sites.

Cation order–disorder relations in end-member amphiboles are of particular interest, as the simple compositions place severe constraints on possible site-populations. To this end, we have put some effort into trying to synthesize crystals of fluor-pargasite of a size sufficient for single-crystal structure refinement; the results of this work are presented here.

Experimental

Synthesis

Forty mg of starting materials (fused silica glass, γ–Al_2O_3, CaF_2, Na_2CO_3, MgO) were sealed in a 4 × 23 mm Pt tube and placed in a conventional vertical quench furnace. The run was held at 1240°C for 1 h and then cooled to 816°C over a period of 332 h. Further experimental details are given by Raudsepp *et al.* (1991).

In general, the run products were more than 90% amphibole, with minor forsterite, plagioclase, clinopyroxene and cristobalite. One run gave crystals up to ~100 μm long with minor fine-grained non-amphibole phases; crystals from this run were used in the present study.

X-ray data collection

Crystals were mounted on a Philips PW–1100 four-circle diffractometer and examined with graphite-monochromatized Mo$K\alpha$ X-radiation; crystal quality was assessed *via* the profile and width of Bragg diffraction peaks. Unit-cell dimensions were calculated from least-squares refinement of the *d* values obtained from 50 rows of the reciprocal lattice by measuring the centroid of gravity of each reflection and of the corresponding antireflection in the θ range between –30 and +30°. Intensity data were collected for the monoclinic equivalent pairs (*hkl* and $h\bar{k}l$) in the θ range $2 < \theta < 30°$. Intensities were then corrected for absorption, Lorentz and polarization effects, averaged and reduced to structure factors. Reflections with $I \geq 5\sigma(I)$ were considered as observed during the structure refinement.

Structure refinement

Structure-refinement procedures were as described in Oberti *et al.* (1992) following the model of Ungaretti (1980). Refinement information and final

TABLE 1. MISCELLANEOUS INFORMATION FOR FLUOR-PARGASITE

	FP(1)	FP(2)		FP(1)	FP(2)
Space group	*C*2/*m*	*C*2/*m*	Crystal size (mm)	0.10 x 0.24 x 0.10	0.12 x 0.26 x 0.14
a (Å)	9.820(4)	9.808(2)	Total Ref.	1356	1361
b (Å)	17.896(6)	17.868(5)	[I(obs) > 2.5σ(I)]	1033	1085
c (Å)	5.294(2)	5.297(2)			
β (°)	105.30(3)	105.30(2)	Final *R*(all)	2.5%	2.1%
V (Å^3)	897.4(3)	895.4(2)	Final *R*(obs)	1.3%	1.2%

Ideal cell contents: $2[NaCa_2Mg_4AlSi_6Al_2O_{22}F_2]$

Analyzed cell contents: FP(1) $2[Na_{0.855}Ca_{2.044}Mg_{4.388}Al_{0.773}(Si_{5.962}Al_{2.038})O_{22}F_2]$
FP(2) $2[Na_{0.809}Ca_{2.228}Mg_{4.217}Al_{0.938}(Si_{5.800}Al_{2.200})O_{22}F_2]$

$R = \Sigma(|F_o|-|F_c|)/\Sigma|F_o|$

TABLE 2. FINAL POSITIONAL PARAMETERS AND EQUIVALENT ISOTROPIC DISPLACEMENT PARAMETERS ($Å^2 \times 10^4$) FOR FLUOR-PARGASITE

	x	y	z	$B_{equiv.}$
O(1)	*0.1069	0.0871	0.2167	0.71
	0.1064	0.0879	0.2155	0.71
O(2)	0.1185	0.1722	0.7357	0.69
	0.1183	0.1726	0.7377	0.69
O(3)	0.1044	0	0.7123	0.77
	0.1044	0	0.7120	0.73
O(4)	0.3670	0.2517	0.7898	0.89
	0.3678	0.2523	0.7904	0.91
O(5)	0.3527	0.1406	0.1146	0.95
	0.3536	0.1414	0.1168	0.95
O(6)	0.3460	0.1167	0.6112	0.98
	0.3456	0.1165	0.6134	0.98
O(7)	0.3446	0	0.2771	1.01
	0.3442	0	0.2762	1.03
T(1)	0.2821	0.0854	0.3043	0.44
	0.2821	0.0856	0.3049	0.44
T(2)	0.2913	0.1733	0.8147	0.48
	0.2917	0.1736	0.8163	0.49
M(1)	0	0.0894	1/2	0.51
	0	0.0897	1/2	0.50
M(2)	0	0.1754	0	0.50
	0	0.1754	0	0.54
M(3)	0	0	0	0.47
	0	0	0	0.48
M(4)	0	0.2794	1/2	0.74
	0	0.2797	1/2	0.70
M(4′)	0	0.2536	1/2	0.89
	0	0.2587	1/2	1.17
A	0	1/2	0	4.04
	0	1/2	0	3.67
A(*m*)	0.0401	1/2	0.0944	2.85
	0.0432	1/2	0.0958	2.69
A(2)	0	0.4713	0	2.00
	0	0.4713	0	1.33

* FP(1) upper line, FP(2) lower line

R values are given in Table 1. Atomic positions and isotropic displacement factors are given in Table 2, refined scattering powers in Table 3, and selected interatomic distances and angles in Table 4; structure factors may be obtained from the Depository of Unpublished Data, CISTI, National Research Council of Canada, Ottawa, Ontario K1A 0S2.

Electron-microprobe analysis

Following collection of the X-ray intensity data, the crystals were mounted in epoxy, polished, carbon-coated and analyzed with a fully automated Cameca SX–50 electron microprobe according to the procedure of Raudsepp *et al.* (1991). As a control on accuracy, diopside and forsterite of known compositions were analyzed at the same time; these showed close agreement with the nominal compositions. Ten points were analyzed on each crystal, and the average compositions are given in Table 5. Unit formulae were calculated on the basis of 23 equivalent oxygen atoms. The analyzed F values (~4.7 wt%) are equal to the nominal value (4.5 wt%) within their standard deviations.

TABLE 3. REFINED SITE-SCATTERING VALUES (ELECTRONS PER FORMULA UNIT) AND EQUIVALENT ELECTRONS (EMP) FROM THE UNIT FORMULAE OF TABLE 5

	FP(1)	FP(2)
M(1)	24.0	24.0
M(2)	25.5	25.3
M(3)	12.0	12.0
Σ[*M*(1),*M*(2),*M*(3)]	61.5	61.3
EMP [*M*(1),*M*(2),*M*(3)]	60.8	60.9
M(4)+*M*(4′)	39.5	39.5
EMP *M*(4)	39.2	39.1
A	12.6	12.9
EMP *A*	12.3	12.8

TABLE 4. SELECTED INTERATOMIC DISTANCES (Å) AND ANGLES (°) FOR FLUOR-PARGASITE*

	FP(1)	FP(2)		FP(1)	FP(2)
T(1)–*O*(1)	1.659	1.663	*M*(2)–*O*(1) x2	2.069	2.052
T(1)–*O*(5)	1.683	1.686	*M*(2)–*O*(2) x2	2.043	2.032
T(1)–*O*(6)	1.677	1.681	*M*(2)–*O*(4) x2	1.970	1.955
T(1)–*O*(7)	1.667	1.669	<*M*(2)–*O*>	2.027	2.013
<*T*(1)–*O*>	1.672	1.675			
			M(3)–*O*(1) x4	2.053	2.056
T(2)–*O*(2)	1.637	1.642	*M*(3)–*O*(3) x2	2.048	2.050
T(2)–*O*(4)	1.609	1.614	<*M*(3)–*O*>	2.051	2.054
T(2)–*O*(5)	1.649	1.651			
T(2)–*O*(6)	1.666	1.666	*M*(4)–*O*(2) x2	2.413	2.412
<*T*(2)–*O*>	1.641	1.643	*M*(4)–*O*(4) x2	2.330	2.330
			M(4)–*O*(5) x2	2.597	2.576
M(1)–*O*(1) x2	2.046	2.048	*M*(4)–*O*(6) x2	2.561	2.564
M(1)–*O*(2) x2	2.083	2.087	<*M*(4)–*O*>	2.475	2.470
M(1)–*O*(3) x2	2.066	2.067			
<*M*(1)–*O*>	2.065	2.067	*A*–*O*(5) x4	3.042	3.049
			A–*O*(6) x4	3.041	3.031
A(*m*)–*O*(5) x2	3.136	3.156	*A*–*O*(7) x4	2.379	2.379
A(*m*)–*O*(5) x2	3.046	3.046	<*A*–*O*>	2.909	2.907
A(*m*)–*O*(6) x2	2.669	2.648			
A(*m*)–*O*(7)	2.366	2.389	*A*(2)–*O*(5) x2	2.633	2.640
A(*m*)–*O*(7)	3.219	3.216	*A*(2)–*O*(6) x2	2.714	2.705
A(*m*)–*O*(7)	2.515	2.501	*A*(2)–*O*(7) x2	2.434	2.433
<*A*(*m*)–O>	2.867	2.867	<*A*(2)–O>	2.594	2.592
O(5)–*O*(6)–*O*(5)	161.5	160.7			
T(1)–*O*(5)–*T*(2)	132.7	132.2			
T(1)–*O*(6)–*T*(2)	136.7	136.8			
T(1)–*O*(7)–*T*(1)	132.8	133.0			

* standard deviations are ≤1 in the last digit

TABLE 5. RESULTS OF ELECTRON-MICROPROBE ANALYSIS OF SYNTHETIC FLUOR-PARGASITE

	FP(1)	FP(2)
SiO_2 wt%	42.19	41.18
Al_2O_3	16.88	18.91
MgO	20.83	20.09
CaO	13.59	13.74
Na_2O	3.12	2.96
F	4.80	4.54
O≡F	-2.02	-1.91
Sum	99.29	99.50
Si	5.962	5.800
Al	2.038	2.200
Sum	8.000	8.000
Al	0.773	0.938
Mg	4.388	4.217
Sum	5.161	5.155
Mg	0.161	0.155
Ca	2.044	2.073
Sum	2.205	2.228
Ca	0.205	0.228
Na	0.855	0.808
Sum	1.060	1.036
F	2.145	2.022

Discussion

Although the nominal composition of the synthesized crystals is end-member fluor-pargasite, electron-microprobe analysis shows them to deviate slightly from this composition. The site populations in these crystals are of particular interest. First, the composition is simpler than most natural amphiboles, and there should be close agreement with established site-population and stereochemical relations. Second, these compositions provide an opportunity to examine *A*-cation positional disorder (Hawthorne & Grundy 1972, Hawthorne 1983) for a simple *A*-site chemistry with $^{[4]}$Al present and only F at the *O*(3) position. Third, there has been considerable recent work on both natural (Oberti *et al.* 1995a) and synthetic pargasite (Raudsepp *et al.* 1987, Welch *et al.* 1994, Jenkins & Hawthorne 1995).

The *C*- and *T*-group cations are Mg, Al and Si, with atomic numbers of 12, 13 and 14, respectively. These scatter X rays in a very similar fashion, and hence site-scattering refinement cannot be used directly to obtain site populations. However, these cations are of very different size ($^{[6]}$Mg = 0.72, $^{[6]}$Al = 0.535, $^{[4]}$Al = 0.39, $^{[4]}$Si = 0.26 Å; Shannon 1976), and the mean bond-lengths thus can be used to derive the site populations.

T(1) and T(2) sites

The <*T*(1)–O> distances indicate 1.90 and 2.00 Al apfu (atoms per formula unit) at the *T*(1) site in FP(1) and FP(2), respectively; these values are significantly less than the amount of $^{[4]}$Al indicated by electron-microprobe analysis, suggesting that some Al occurs at the *T*(2) site. Direct estimation of the Al content of *T*(2) from the <*T*(2)–O> distance is less straightforward than the analogous problem for the *T*(1) tetrahedron, as there is significant evidence to indicate that <*T*(2)–O> is inductively affected by the *M*(4) occupancy, the Fe content of the octahedral sites, and possibly the occupancy of the *A* site. Synthetic fluor-edenite (Boschmann *et al.* 1994) has the same *M*(4) and *A*-site occupancies as fluor-pargasite, and both lack Fe. Synthetic fluor-edenite and fluor-pargasite have <*T*(2)–O> distances of 1.635 and 1.642 Å, respectively, again indicating that there is significant Al at *T*(2) in synthetic fluor-pargasite. Using our unpublished regression curve for the <*T*(2)–O> bond-length, Al contents of 0.09 and 0.12 apfu are predicted for the *T*(2) site in crystals FP(1) and FP(2), respectively. This partial disorder of Al over *T*(1) and *T*(2) is in line with the ^{29}Si MAS NMR results of Raudsepp *et al.* (1987) on scandium-fluor-pargasite. In addition, it correlates with the behavior of $^{[4]}$Al in natural amphiboles, as high-temperature parageneses do contain amphiboles with significant $^{[4]}$Al disorder, whereas low-temperature parageneses contain amphiboles with $^{[4]}$Al ordered at the *T*(1) site (Oberti *et al.* 1995b).

The M(1), M(2) and M(3) sites

We have refined a large number (~650) of monoclinic amphibole structures, and are continually re-examining the relations between metric (cell dimensions, bond lengths, bond angles) and chemical (bulk composition, site populations) characteristics of the amphibole structure. Recently, we noticed that the <*M*–O> bond-lengths in pargasitic amphiboles seem to behave differently from the analogous bond-lengths in other amphiboles: the observed <*M*(1)–O> distances are longer and the <*M*(3)–O> distances are shorter than we would predict on the basis of site populations at the *M* and *O*(3) sites. This point was examined in detail by Oberti *et al.* (1995a), who showed that in Fe-poor pargasite from an ultramafic environment, there is significant Al (up to 0.32 apfu) at the *M*(3) site and no Al at the *M*(1) site. This disorder of Al over the *M*(2) and *M*(3) sites in Fe-poor pargasite is in accord with the infrared and ^{1}H MAS NMR spectra of synthetic pargasite (Raudsepp *et al.* 1987, Welch *et al.* 1994), which indicate Al disorder over the octahedrally coordinated *M* sites. The amphiboles examined by Oberti *et al.* (1995a) are essentially F-free, as are the synthetic pargasite samples of

TABLE 6. OBSERVED AND CALCULATED <*M*–O> DISTANCES (Å) IN SYNTHETIC FLUOR-PARGASITE CRYSTALS, ASSUMING ALL $^{[6]}$Al AT *M*(2)

	FP(1)		FP(2)	
	OBS.	CALC.	OBS.	CALC.
M(1)	2.067	2.052	2.065	2.052
M(2)	2.013	2.011	2.027	2.023
M(3)	2.054	2.052	2.051	2.052

Raudsepp *et al.* (1987) and Welch *et al.* (1994). Does F have an effect on the pattern of $^{[6]}$Al order in pargasite? This question is resolved by the present work.

Both synthetic fluor-pargasite crystals deviate significantly from ideal stoichiometry (Table 5). Thus there are two questions to consider: (1) are the unit formulae derived from the electron-microprobe data compatible with the refined structures; (2) what is the pattern of order of $^{[6]}$Al in these crystals? Because of the constrained nature of these problems, we can answer both of them by the same calculation. If we assume that all $^{[6]}$Al is ordered at *M*(2), our latest predictive curves give the <*M*–O> distances shown in Table 6. There is close agreement for the *M*(2) site with all $^{[6]}$Al ordered at *M*(2), and there is also virtually exact agreement for the *M*(3) site with no $^{[6]}$Al at *M*(3). Any attempt to disorder $^{[6]}$Al between *M*(2) and *M*(3) will lead to worse agreement between the observed and calculated <*M*(2)–O> and <*M*(3)–O> distances. Moreover, these distances are compatible with the amounts of *C*-group Al indicated by the unit formulae (Table 5). There is a significant discrepancy between the observed and predicted <*M*(1)–O> distances (Table 6), a matter of 0.014 Å for *both* crystals. As the observed distances are longer than the calculated distances, assignment of $^{[6]}$Al to *M*(1) would exacerbate this discrepancy, and thus we may conclude that there is no $^{[6]}$Al at *M*(1). Hence we may conclude that $^{[6]}$Al is completely ordered at *M*(2) in these fluor-pargasite crystals, and that the $^{[6]}$Al calculated from the electron-microprobe data is completely compatible with the observed bond-lengths. Note that this pattern of order is the same as that for Sc and Cr^{3+} in synthetic scandium- and chromium-fluor-pargasite (Raudsepp *et al.* 1987).

The reason for the discrepancy in observed and predicted <*M*(1)–O> distances is not clear. There are three possibilities: (1) there is some Ca at *M*(1), (2) there is some Na at *M*(1), or (3) there is an inductive effect that is particularly effective in pargasite and that our predictive curves do not model. The refined scattering at *M*(1) (Table 3) is not compatible with significant Ca at *M*(1). To increase the predicted <*M*(1)–O> distance by 0.014 Å would require 0.10 apfu of Ca at *M*(1); this would give an *M*(1) scattering of 24.8 epfu (electrons per formula unit). This value is significantly larger than the refined values of 24.0 epfu (Table 3), and so possibility (1) can be discounted. On the other hand, the refined scattering at *M*(1) is compatible with Na at *M*(1), as the scattering powers of Mg ($Z = 12$) and Na ($Z = 11$) are very similar. To increase the predicted <*M*(1)–O> distance by 0.014 Å would require 0.09 apfu of Na at *M*(1). This would displace a corresponding amount of Mg to the *M*(4) site, and increase the discrepancy between the refined amount of Mg at *M*(4) (~0.06 apfu) and the amount assigned from the formula unit (0.16 + 0.09 = 0.25 Mg apfu). This discrepancy suggests that possibility (2) does not occur. In addition, unpublished work suggests that *C*-group Ca and Na order at the *M*(3) site. Is there an inductive mechanism that is particularly effective in increasing the <*M*(1)–O> bond-length in pargasitic amphiboles? The results of Oberti *et al.* (1995a) suggest that this is the case; however, the details of this are still obscure.

M(4) site

The unit formulae calculated from the results of electron-microprobe analysis both have excess *C*-group cation values of Mg (0.16 apfu, Table 5), and the presence of appreciable density at the *M*(4)′ site also indicates significant *B*-group Mg. Refinement of the total scattering at the *M*(4) site gave a value of 39.50 epfu, indicating an Mg content at *M*(4) of ~0.06 apfu, approximately one-third the value derived by electron-microprobe analysis. Thus there is a slight disagreement in these two values, but both indicate significant occupancy of *M*(4) by Mg. Moreover, there is a slight excess of total cations (0.06 and 0.04 apfu, respectively) in the unit formulae, indicative of error in the microprobe analysis or in the renormalization procedure. Reduction of the overall cation sum to the maximum possible value of 16 apfu produces closer agreement between the refined Mg contents of *M*(4) and the *B*-group Mg assigned from the electron-microprobe determinations.

The observed <*M*(4)–*O*> distance in synthetic fluor-pargasite, 2.475 Å, is similar to that in synthetic fluor-edenite, but significantly larger than that in synthetic fluor-tremolite, 2.459 Å (Cameron & Gibbs 1973), in which *M*(4) also is occupied by Ca. This difference is inductively caused by stereochemical differences in the rest of the structure (Hawthorne 1983), particularly the presence of the *A* cation in fluor-pargasite and fluor-edenite.

The A(m) and A(2) sites

Much work has been done on this particular aspect of the amphibole structure, as reviewed by Boschmann *et al.* (1994), and factors affecting cation order at the *A* site are considered in detail by Hawthorne *et al.*

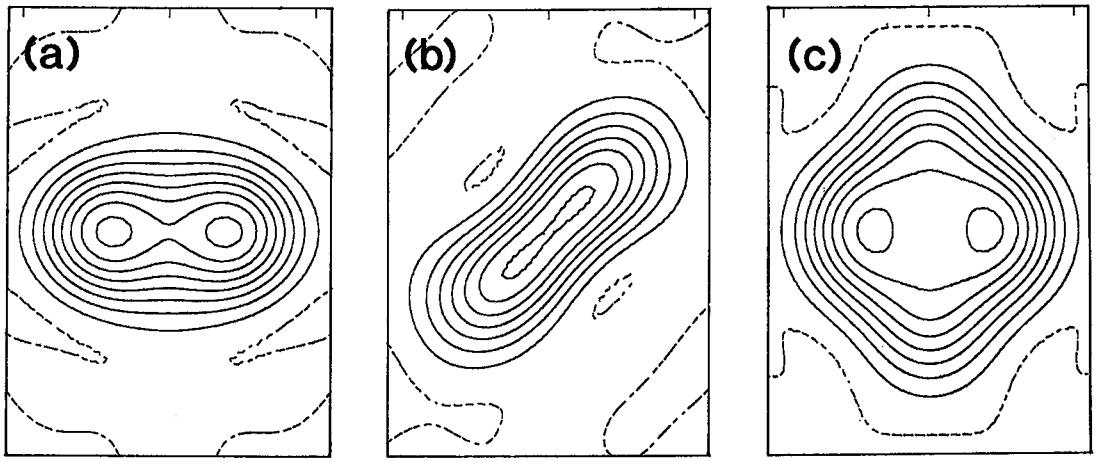

FIG. 1. Difference-Fourier sections for synthetic fluor-pargasite FP(1), calculated through the central $A(2/m)$ site with the A cation removed from the structural model: (a) (100) section at $x = 0$ with [010] horizontal; (b) (010) section at $y = ½$ with c horizontal; (c) section through the electron-density maxima on the 2-fold axis and in the mirror plane, approximately parallel to $(\bar{2}01)$ with [010] horizontal; the contour interval is 1 e/Å^3.

(1995). Figure 1 shows various difference-Fourier maps through the $A(2/m)$ position for synthetic fluor-pargasite FP(1), calculated with the A cations removed from the refinement model. There is significant electron-density both along the 2-fold axis (Fig. 1a) and in the mirror plane (Fig. 1b). A section through $(\bar{2}01)$, the plane of maximum electron-density, shows the overall distribution of electron density in the A cavity (Fig. 1c), and indicates that the maximum electron-density occurs on the 2-fold axis, at the $A(2)$ position. The separation of the two maxima along the 2-fold axis is approximately 0.7 Å, the wavelength of the X radiation used to collect the diffraction data, and the separation of the $A(2)$ and $A(m)$ positions is of similar magnitude. The limit of resolution of diffraction data is normally taken to be 0.7 λ, and we are close to this limit in the present situation. Consequently, the details of the A-site occupancies are not well resolved, although Figure 1c does require that the scattering be higher at $A(2)$ than at $A(m)$. In an effort to circumvent this problem, we fixed the $A(2)$ position at the maximum electron-density position in Figure 1c, and refined the positional parameters of $A(m)$ plus the site scattering at $A(m)$ and $A(2)$. Subsequent difference-Fourier maps showed significant residual electron-density on the 2-fold axis, displaced from the main $A(2)$ site. A second $A(2')$ site was introduced into the refinement, with its y coordinate fixed at the position of the residual maximum in the difference-Fourier map. Subsequent refinement showed significant scattering from this site. However, any attempt to release the $A(2)$ and $A(2')$ positions resulted in the refinement becoming unstable.

We must accept the fact that we cannot derive quantitative information on A-site configurations in fluor-pargasite. The sequence of refinement steps indicates that there are at least two different $A(2)$ sites, and perhaps a range of y values for the cation(s) occupying the $A(2)$ site(s). The same inference may also apply to the $A(m)$ site, but the lower occupancy at $A(m)$ means that any positional disorder at $A(m)$ is less well defined than at $A(2)$. Combined with the fact that both Ca and Na occur at the A site, this complexity means that X-ray scattering lacks the resolution to come up with a unique solution. However, we can get a qualitative idea of the site occupancy. All models used for the A site resulted in significantly greater electron-density at $A(2)$ than at $A(m)$ (Fig. 1c). Characterization of cation ordering at the A site in K-free amphiboles of different composition (Hawthorne *et al.* 1995) shows that Na tends to order at the $A(m)$ site in F-rich amphiboles. The occurrence of at least two $A(2)$ positions suggests that these synthetic fluor-pargasite crystals have Ca ordered at the $A(2)$ site, but quantitative evaluation of occupancies is not possible. However, we do note that the model with all available A-site Ca at $A(2)$ means that Na is (approximately) equally split between $A(2)$ and $A(m)$, as was found in synthetic fluor-edenite (Boschmann *et al.* 1994).

CONCLUSIONS

1. Tetrahedrally coordinated Al is strongly ordered at $T(1)$ ($^{T(1)}$Al ≈ 2.0 apfu), but significant Al occupancy of $T(2)$ does occur ($^{T(2)}$Al ≈ 0.10 apfu) in these synthetic fluor-pargasite crystals.

2. Octahedrally coordinated Al is ordered at $M(2)$. This is similar to the $^{[6]}M^{3+}$ ordering observed in synthetic scandium- and chromium-fluor-pargasites by Rietveld structure refinement (Raudsepp *et al.* 1987), and contrasts with the $^{[6]}M^{3+}$ disorder observed by infrared spectroscopy in synthetic pargasite (Raudsepp *et al.* 1987) and by single-crystal structure refinement of pargasite (Oberti *et al.* 1995a). Thus we may conclude that the identity of the $O(3)$ anion (*i.e*, OH *versus* F) greatly affects the pattern of order of Mg–Al over the $M(1)$, $M(2)$ and $M(3)$ sites in pargasite.
3. Both Na and Ca occur at the A site in the crystals examined. Detailed occupancies of the $A(m)$ and $A(2)$ sites could not be derived, but the pattern of electron density suggests that Na is disordered between $A(m)$ and $A(2)$, and that Ca occurs predominantly at $A(2)$.

Acknowledgements

We thank George Guthrie and an anonymous reviewer for their comments. Financial support was provided by the Natural Sciences and Engineering Research Council of Canada in the form of Operating, Major Equipment and Infrastructure grants to FCH, a Killam Fellowship to FCH, and by CNR-NATO.

References

Boschmann, K.F., Burns, P.C., Hawthorne, F.C., Raudsepp, M. & Turnock, A.C. (1994): A-site disorder in synthetic fluor-edenite: a crystal-structure study. *Can. Mineral.* **32**, 21-30.

Cameron, M. & Gibbs, G.V. (1973): The crystal structure and bonding of fluor-tremolite: a comparison with hydroxyl tremolite. *Am. Mineral.* **58**, 879-888.

Charles, R.W. (1980): Amphiboles on the join pargasite–ferropargasite. *Am. Mineral.* **65**, 996-1001.

Hawthorne, F.C. (1983): The crystal chemistry of the amphiboles. *Can. Mineral.* **21**, 173-480.

_____ & Grundy, H.D. (1972): Positional disorder in the *A*-site of clino-amphiboles. *Nature Phys. Sci.* **235**, 72-73.

_____, Oberti, R. & Sardone, N. (1995): Ordering at the A site in clinoamphiboles: the effects of composition on ordering patterns. *Eur. J. Mineral.* (in press).

Jenkins, D.M. & Hawthorne, F.C. (1995): Synthesis and Rietveld refinement of amphiboles along the join $Ca_2Mg_5Si_8O_{22}F_2 - NaCa_2Mg_4Ga_3Si_6O_{22}F_2$. *Can. Mineral.* **33**,

Oberti, R., Hawthorne, F.C., Ungaretti, L. & Cannillo, E. (1995a): $^{[6]}$Al disorder in amphiboles from mantle peridotites. *Can. Mineral.* **33** (in press).

_____, Ungaretti, L., Cannillo, E. & Hawthorne, F.C. (1992): The behaviour of Ti in amphiboles. 1. Four- and six-coordinate Ti in richterite. *Eur. J. Mineral.* **4**, 425-439.

_____, _____, _____, _____ & Memmi, I. (1995b): Temperature-dependent Al order-disorder in the tetrahedral double-chain of *C2/m* amphiboles. *Eur. J. Mineral.*

Raudsepp, M., Turnock, A.C. & Hawthorne, F.C. (1991): Amphibole synthesis at low pressure: what grows and what doesn't. *Eur. J. Mineral.* **3**, 983-1004.

_____, _____, _____, Sherriff, B.L. & Hartman, J.S. (1987): Characterization of synthetic pargasitic amphiboles ($NaCa_2Mg_4M^{3+}Si_6Al_2O_{22}(OH,F)$; M^{3+} = Al,Cr,Ga,Sc,In) by infrared spectroscopy, Rietveld structure refinement and ^{27}Al, ^{29}Si and ^{19}F MAS NMR spectroscopy. *Am. Mineral.* **72**, 580-593.

Robinson, K., Gibbs, G.V., Ribbe, P.H. & Hall, M.R. (1973): Cation distribution in three hornblendes. *Am. J. Sci.* **273A**, 522-535.

Shannon, R.D. (1976): Revised effective ionic radii and systematic studies of interatomic distances in halides and chalcogenides. *Acta Crystallogr.* **A32**, 751-767.

Ungaretti, L. (1980): Recent developments in X-ray single crystal diffractometry applied to the crystal-chemical study of amphiboles. *God. Jugosl. Cent. Kristalogr.* **15**, 29-65.

Welch, M.D., Kolodziejski, W. & Klinowski, J. (1994): A multinuclear NMR study of synthetic pargasite. *Am. Mineral.* **79**, 261-268.

Westrich, H.R. & Navrotsky, A. (1981): Some thermodynamic properties of fluorapatite, fluorpargasite, and fluorphlogopite. *Am. J. Sci.* **281**, 1091-1103.

Received March 8, 1994, revised manuscript accepted August 5, 1994.